# Design and development of a low-cost floater for sustainable fishing

**(SOUND (Schmidt Marine Foundation, Global Fisheries Tech Initiative) andHorizon Europe under the UWIN-LABUST project (101086340).)**

**Babić, Anja; Oreč, Martin; Mišković, Nikola; Dahan, Shlomi; Vonić, Marijan; Sidaropoulos, Iwan; Cukrov, Neven; Diamant, Roee**

# Design and development of a low-cost floater for sustainable fishing

Anja Babić , *Member, IEEE*, Martin Oreč Nikola Mišković , *Senior Member, IEEE*, Shlomi Dahan, Marijan Vonić, Iwan Sidaropoulos, Neven Cukrov, Roee Diamant , *Senior Member, IEEE*

**Abstract**

While it is widely recognized that fish are an ecologically and commercially important group, our current knowledge of fish occurrence, composition (diversity), abundance and behavior (e.g. migration) is limited to anecdotal sightings and reports, often from laypersons. In situ marine monitoring bridges this gap and allows us to track and monitor marine life. One such system is the SOUND system: a swarm of low-cost Lagrangian floats that can non-invasively support aquaculture and fisheries, especially in remote areas and developing countries. The swarm of floats works together in a group and uses underwater acoustic communication. It provides long-term data on the fish population, which can shed light on the interdependencies of spatially segmented ecosystems, the top-down regulation of bio-geophysical processes and the sensitivity of the environment to anthropogenic stress factors. SOUND Floater consists of a piston-based buoy control system, an active sonar system with on-board analysis and a satellite communication module. It is capable of probing the water to a depth of 50 m while maintaining position with an accuracy of $<$10 cm, detecting schools of fish from a distance of 500 m and operating for 5 consecutive days. In this technical communication paper we present the detailed design of the SOUND prototype, including its mechanical, electrical and algorithmic parts. We report on results from laboratory pool and from two sea trials.

Anja Babić, Martin Oreč, Nikola Mišković, Marijan Vonić and Roee Diamant are with the Faculty of Electrical Engineering and Computing, University of Zagreb, Croatia. Shlomi Dahan and Roee Diamant are with Hatter Department of Marine Technologies, University of Haifa, Israel. Iwan Sidaropoulos is with Polytech Montpellier, France. Neven Cukriv is with the division for marine and environmental research, Ruder Bošković Institute, Croatia. (Corresponding author email: roee.d@univ.haifa.ac.il).

Part of this work has been presented in the Oceans conference, Singapore, April, 2024. This journal version extended the conference publication by adding: 1) extended description of the electronics and acoustic components, 2) a revised design for the mechanical parts of the system, 3) results from two sea experiments, 4) explanation about the communication scheme of the floater. This work was sponsored in part by the Schmidt Marine Foundation via the Global Fisheries Tech Initiative, and by the European Union's Horizon Europe programme under the UWIN-LABUST project (project no. 101086340).

**Index Terms**

Lagrangian floater, marine monitoring, depth control, vehicle design, underwater acoustics, target tracking

## I. Introduction

It is well known that fish are an important group both ecologically and commercially. Nevertheless, our knowledge of fish occurrence, composition, abundance and behavior is often limited to anecdotal sightings and reports, often obtained through invasive techniques such as net catches [1]. In this context, in situ marine monitoring, which allows remote monitoring of fish, can improve our knowledge of the presence and behavior of important fish populations. This includes increasing our knowledge of fish movements and abundance and understanding behaviors such as schooling, cohesiveness, and vessel avoidance. Monitoring fish populations will also enable efficient management of important commercial activities on the coast, in particular reducing bycatch by fisheries and promoting data-driven decision making in marine research [2]. Assessment of marine fauna must be based on efficient and preferably autonomous surveys to create large, labeled databases [3], and data must be correlated across time and space [4]. In developing countries, the main source of information on fish biomass comes from catch analysis due to a lack of government monitoring; therefore, an independent assessment is required. To this end, we have developed an autonomous system that performs on-the-fly monitoring of fish schools. This is the SOUND system.

The SOUND project designs a swarm of low-cost Lagrangian floats that drift with the water current and simultaneously perform active acoustic fish detection and on-site fish biomass assessment (Fig. 1). The result provides spatial information on the location, school size and biomass of the fish. The system provides long-term data on the fish population, which sheds light on the interdependencies of spatially segmented ecosystems, the top-down regulation of bio-geophysical processes as well as the environment and sensitivity to anthropogenic stressors. This will provide a comprehensive overview of the state of the food web in terms of biomass and reflect the current state of functioning of the marine ecosystem under study. Such an insight will provide a quantitative tool for reviewing management and planning efforts in relation to marine space. Especially in remote areas and in developing countries where advanced means of

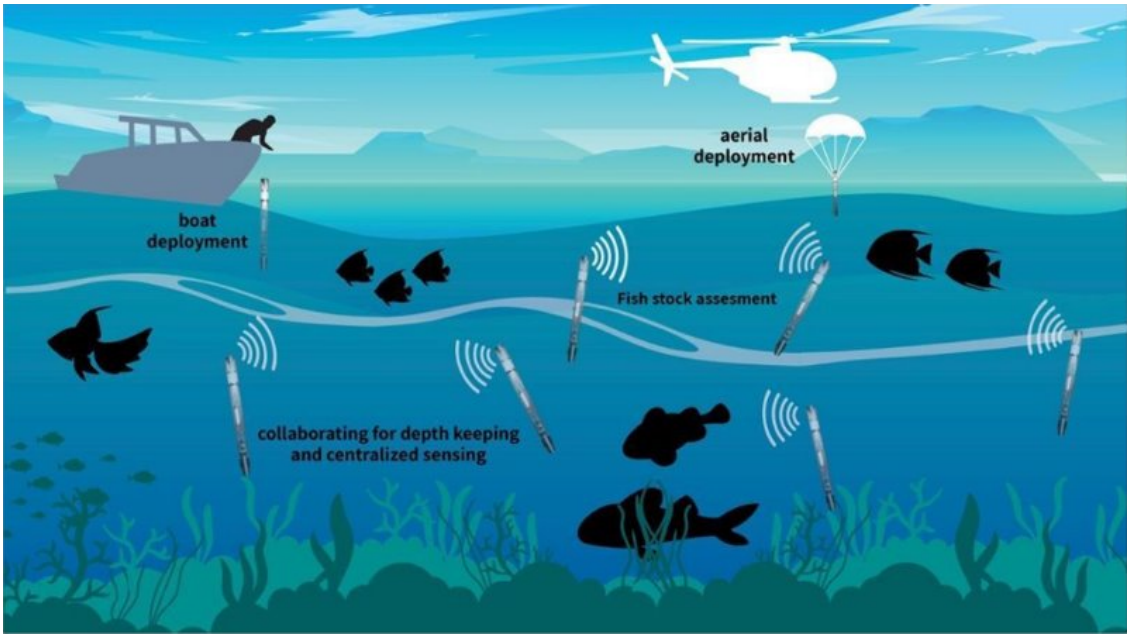


Fig. 1: Illustration of the SOUND system concept.

fish stock assessment are not available, a successful development that is plausible — because it is safe and does not require special permission — will greatly improve the efficiency and quality of geophysical surveys. SOUND's capabilities will also benefit natural authorities by enabling them to properly guide and direct the local fishing industry. On a broader scale, SOUND can contribute to ecosystem monitoring by providing real-time tagged data on pelagic fish. Visual information can be found at [5].

SOUND floaters can profile the water column to a depth of 50 m or maintain the depth in cm resolution. Using an areal array, acoustic detection tracks individual fish up to a distance of 500 m and can relay information to other floaters up to a distance of 1 km. The system is designed to be energy efficient and can operate for up to 5 days. Information from multiple floats is exchanged via underwater acoustic communication and translated into the spatial distribution of fish; data that is currently only available from models. Once a joint decision has been made, the floaters can surface and transmit their results via satellite communication. The floaters are small and lightweight. They can be launched by a single person from a small ship. The self-construction of the mechanical, sensory and electrical parts enabled a low-cost development. This technical communication paper describes the technological contribution of the SOUND Floater: its underwater acoustic unit and the mechanism for controlling its buoyancy. The results of two

sea trials in the Red Sea and the Adriatic Sea are presented. Our aim is to support developers of marine monitoring systems by sharing our design information.

The remaining of this paper contains an overview of similar fish monitoring solutions (Section II), a description of the mechanical part of the SOUND floater (Section II-A), an introduction to the electronic components of the floater (Section III) and details about the algorithms of the floater (Section IV). The results of two field trials are given in Section V, and conclusions are drawn in Section VI.

## II. Available Solutions for Fish Monitoring

Abundance indices for highly migratory animals are often based on fishery-dependent data, which are known to be biased towards more sensitive species and certain types of habitat or fishing gear [6]. In addition, fishery records are dependent on an incentive to report and are therefore complicated by the typical omission of illegal, unreported and unregulated (IUU) fishing, as well as discarded catches or catches from recreational [7]. To avoid this type of bias, it is necessary to develop indiscriminate and reliable fishery-independent methods. An alternative to this are dive surveys, in which fish species are visually recorded using a belt transect and the species and individuals are recorded with a camera [8]. However, the area surveyed is limited - both in terms of the area covered by the divers and the range of observation. Furthermore, for safety reasons, dive surveys are only carried out in coastal areas and are virtually non-existent in developing countries. As a result, acoustic systems are increasingly used for remote sensing of marine fauna in ecological surveys [9].

Acoustic remote sensing techniques mostly involve narrow-beam sonar, which can image the water column beneath a survey vessel (a research ship or often a torpedo-shaped Autonomous Underwater Vehicle (AUV)), or a wide-beam sonar array deployed over fixed infrastructures [10]. For example, multibeam echosounders mounted on Autonomous Surface Vehicles (ASV) have been used to survey shipwrecks [11] and to map unique tufa structures [12]. Underwater gliders, characterized by their low cost and long-term deployment potential, use a variety of buoyancy control methods and different acoustic payloads and have proven to be well suited for acoustic surveying [13], [14]. There are two main approaches for detecting targets using acoustic emissions. The first is to transmit pulses with guard intervals inserted to suppress clutter. The target is then found by tracking its possible path after a certain number of acoustic signals have been emitted [15]. However, due to mismatches between the assumed clutter model and

the distribution of reflections from the detected targets, as well as hard assumptions about the target's movement pattern, the current systems are prone to false detections, and robustness for detecting different fish species is still a challenge. The second approach is continuous active SONAR (CAS), which uses narrowband transmissions in multiple subcarriers to detect Doppler components [16]. While the latter approach enables near real-time detection, its energy consumption is too high for small, autonomous vehicles. In addition, the current approach to fish biomass assessment relies on the rather imprecise relationship between acoustic target strength and fish size [17], [18], [19], and no current approach reliably measures the biomass of detected fish in-situ. Current approaches to assess marine biota are limited by the information provided. In particular, current acoustic imaging techniques only detect objects directly beneath a survey vessel and there are no reliable commercial methods for assessing fish biomass. Therefore, there is a need to develop a reliable system for autonomous detection, classification and enumeration of marine species [20]. This can not only improve the efficiency of environmental monitoring tasks, but also pave the way for long-term and far-reaching investigations.

Flotation devices for monitoring the oceans are currently in use worldwide. The best-known devices are the Argo floats [21], which are profiling floats that continuously scan the water column while collecting temperature and salinity measurements. Depth profiling is carried out by a hydraulic pump that inflates or deflates an external bladder. The depth-changing mechanism of EM-APEX floats provides buoyancy control through a combination of an air pump that inflates or deflates an air bladder while a piston simultaneously pushes or draws oil into a reservoir, resulting in a change in average density [22], [23]. The mechanism used by the RAFOS floats [24] controls their depth by adaptively adjusting a ballast weight to achieve buoyancy towards a specific desired depth. Quasi-Lagrangian floats, which control their buoyancy by changing their volume via the movement of two concentric cylinders on top of each other, are described in [25]. However, the continuous acoustic monitoring is impaired by the strong noise emitted by the motor during depth maintenance. Similar limitations exist when using a pump that forces oil through a bladder to change the buoyancy [26], or a thruster for active depth control [27].

The floater described in [28] is designed to have negative buoyancy while thruster operation is scheduled to ascend or descend. To reduce battery consumption and noise, the floater has a parachute-like tarpaulin sheet that opens like an umbrella when the floater descends and closes when it ascends. Another design is that of the aMussel robots [29] whose buoyancy control mechanism consists of a piston and an impenetrable membrane which allows them to float on

the water surface or sink to the seabed. The SOUND floater builds on these designs by being able to passively maintain depth by achieving neutral buoyancy, making it quieter and more efficient operation.

### *A. Mechanical design*

The main body of the SOUND floater consists of a 95 cm long Plexiglas tube, closed at one end by the buoyancy mechanism and at the other end by a cap containing all the required penetrators, switches, probes and active parts of the acoustic devices. The cap is designed to separate into two parts that are relatively movable, as shown in Fig. 2. When the two parts are joined together, the cap is closed and completely seals the top of the cylinder. When the upper part of the cap is opened by a pull and-rotate motion, the user gains direct access to the floater's electronics without having to open the entire system. This can be used for wired battery charging, direct serial communication and general maintenance. Under the upper part of the cap there is a groove for cable glands, sensors and probes so that these do not have to be placed on the top of the device. Four hydrophones are mounted symmetrically on a bracket that radiates outwards from the main body of the floater, while the acoustic projector is mounted on the top of the cap. The mount for the hydrophones also serves as an attachment point for the 1 m long antenna for the GPS and Iridium signal when the floater surfaces for data transmission (Fig. 3).

The depth control mechanism of the SOUND floaters is based on changing the buoyancy of their elongated and bottom-heavy body. The design consists of a single chamber with variable volume and a piston near the bottom of the main body so that the device becomes buoyant as the volume changes. The floater has the greatest volume and buoyancy when the piston is fully extended and the least volume and buoyancy when the piston is fully retracted. The actuator that controls this change is a single piston with a linear drive mechanism and a rolling diaphragm (Fig. 4). A lead screw is used for this linear mechanism as it can generate a large force and thus overcome the high pressures at greater depths. A detailed view of the linear drive mechanism can be found in Fig. 5. In it, a central spur gear is rotated by three other spur gears that are connected to the motors. The nut connection couples the two outer nuts to the central spur gear. The lower nut and the central spur gear are attached directly to the nut connection, while the upper nut is connected via the shaft collar.

The use of several small electric motors coupled together makes it possible to drive the buoyancy system in a float with low power consumption and low voltage, while still ensuring

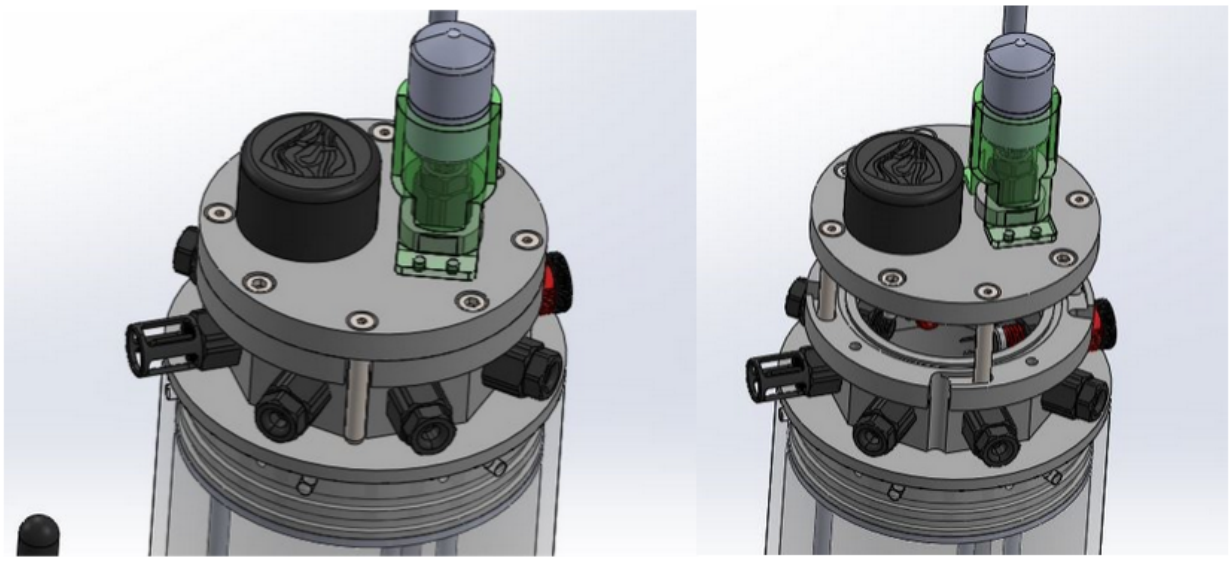

Fig. 2: SOUND floater prototype top cap design, sealed for deployment (left) and open for access (right).

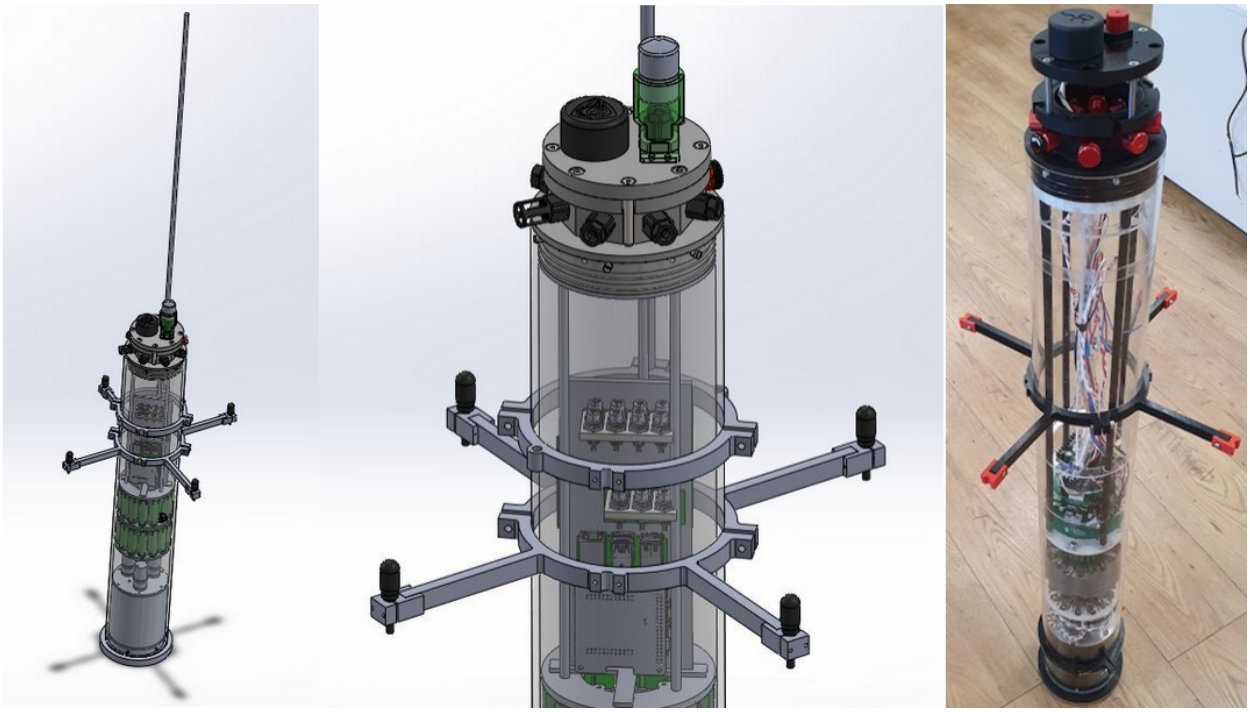

Fig. 3: SOUND floater prototype antenna and hydrophone mount design (left). Full hull prototype with hydrophone mount (right).

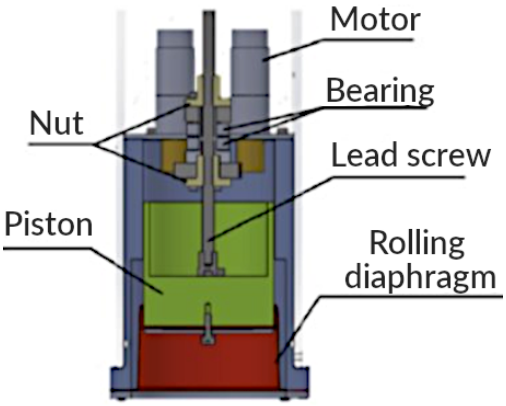


Fig. 4: SOUND floater buoyancy mechanism design cross-section.

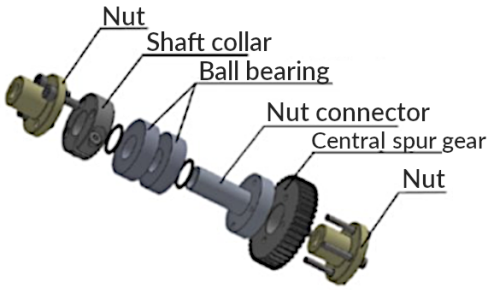


Fig. 5: Detailed view of the linear mechanism design.

high torque and fast actuation. This mechanical system is combined with two limit switches that detect the upper and bottom extreme positions of the piston when touched and activated by the lead screw. A Hall effect quadrature encoder and a pressure sensor enable low complexity control algorithms that allow implementation on low cost electronics. The functionality allows the floaters to maintain a specific depth, profile or surface for reporting or retrieving data. The motors themselves are made quiet by a vibration absorbing material (silicone) that is glued between the motor and the body of the floater. This decouples the motor from the floater enclosure to avoid disturbances to the acoustic unit. The reduction in motor usage during operation also serves to reduce noise and allows better energy efficiency.

Following several laboratory and field tests, the mechanism for controlling the buoyancy of the floater was redesigned to use a stepper motor and a modified gearbox. The use of a single stepper motor instead of coupled DC motors simplifies the control of the piston position as no external position sensor, such as an encoder, is required. The redesigned system contains only

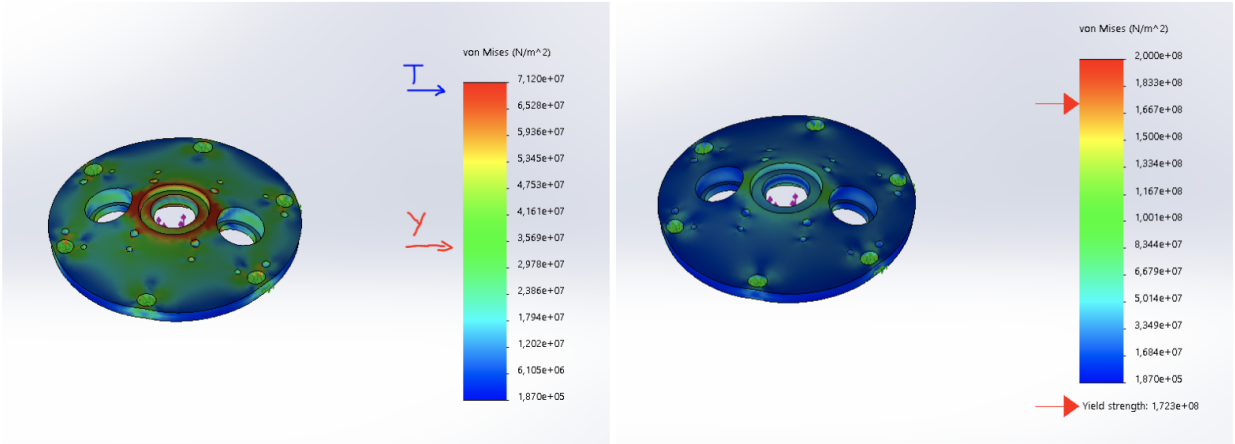


Fig. 6: Finite Element Analysis results of motor holding plate in initial floater design (left), new aluminium alloy version (right).

one limit switch in the center of the piston guide spindle area, which is used for the initial calibration of the piston position. The stepper motor used in the design has been selected so that it can deliver the required torque for surface machining from the maximum allowable depth while keeping current consumption low. The new design also includes a reinforced metal motor support plate structure to compensate for the weaknesses of the previous design (see FEA results in Fig. 6).

The floater reassembled with the new mechanism was tested in a laboratory pressure chamber for depths up to 6 bar to confirm that it is capable of delivering the desired and designed torque and piston speeds (nut torque 2.7 Nm and piston speed 83.65 mm/min).

## III. Electronics Design

The main electronics of the floater are divided into a depth control section and an acoustic detection section. Both have independent power supplies so that the noise-sensitive acoustic detection and processing part is isolated from the part dealing with the motor and buoyancy control. All electronics and battery support skeleton is connected to the top cap. The acoustic sensing section consists of a Raspberry Pi 4 as the main board and includes the entire acoustic data acquisition and processing subsystem, while the general sensing, depth control and communication section uses an atmega32u4-based board (Arduino) to manage acoustic communication between each floater and between the floater and on-surface control via an

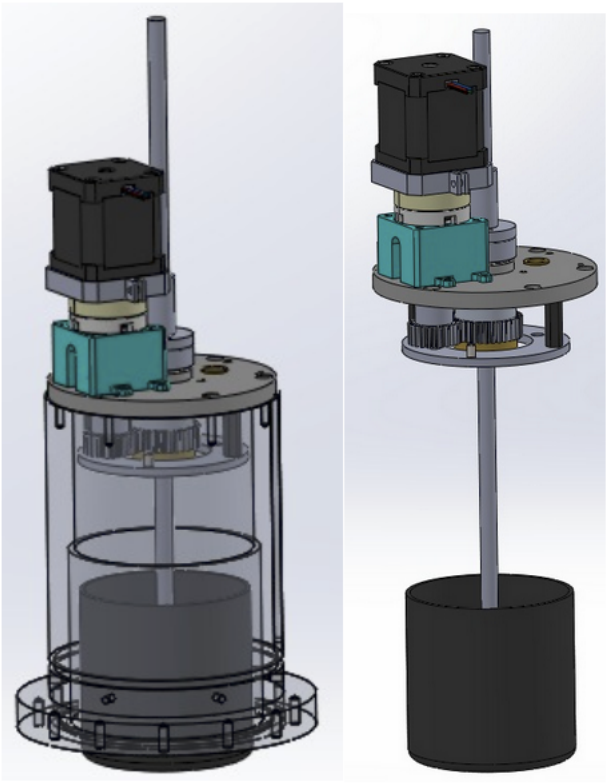

Fig. 7: The redesigned buoyancy mechanism, motors, and gearbox, for stepper motor.

acoustic modem (Nano-modem [30]). The Arduino-controlled part also collects data from the pressure/temperature sensor on the top cap as well as the position encoder and limit switches on the buoyancy mechanism, completing the loop for depth control. A block diagram of the SOUND floater electronics is shown in Fig. 8.

### *A. Acoustic detection subsystem*

The acoustic detection subsystem consists of a projector, four hydrophones, a preamplifier, a sound card and a data processing card. Acoustic transmission is achieved by generating an acoustic signal (a sequence of linear chirps) from the main processor, amplified by the power amplifier and finally transmitted by the piezoelectric element in the frequency range of 30-41KHz. The acoustic reverberations are sampled by 4 hydrophones. Each hydrophone is connected to a preamplifier with 70 dB gain. A four-channel ADC samples the reflections synchronously at 96 ksps at 24 bit per sample. The analysis in the main processor detects targets and calculates

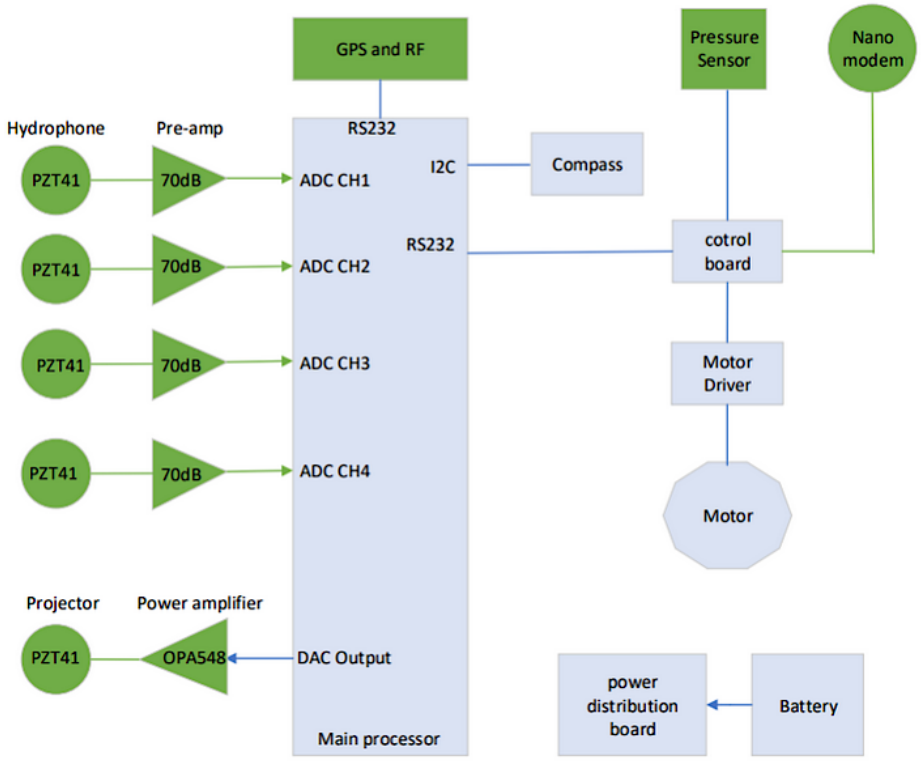


Fig. 8: Block diagram of the SOUND floater electronics.

their trajectories. The results are then transmitted to nearby floaters via the acoustic modem and/or to the user via an Iridium satellite module together with the GPS location of the floater.

*1) Hydrophones:*

The hydrophones were manufactured in-house and are based on the piezoelectric element PZT41 with a size of OD33.7*ID29.9*13.3 mm and a capacitance of 7000pF±12.5%. A supporting network for each element adjusts the impedance of the hydrophone to a frequency of 34 kHz. To fabricate the hydrophone, two wires are soldered to the piezoelectric element with the positive pole of the signal connected to the inside of the element, as shown in Fig. 9. A waterproof polyurethane potting compound UR5041 is used for potting the hydrophone and the electronics. This resin system was selected due to its exceptional resistance to salt water. Using a template frame, care is taken to ensure that the piezoelectric element remains free during potting and does not come into contact with other components. To avoid bubbles in the potting compound, the element is then vacuumed for several minutes. The potting process is shown in Fig. 9, and a finished hydrophone unit can be seen in Fig. 10.

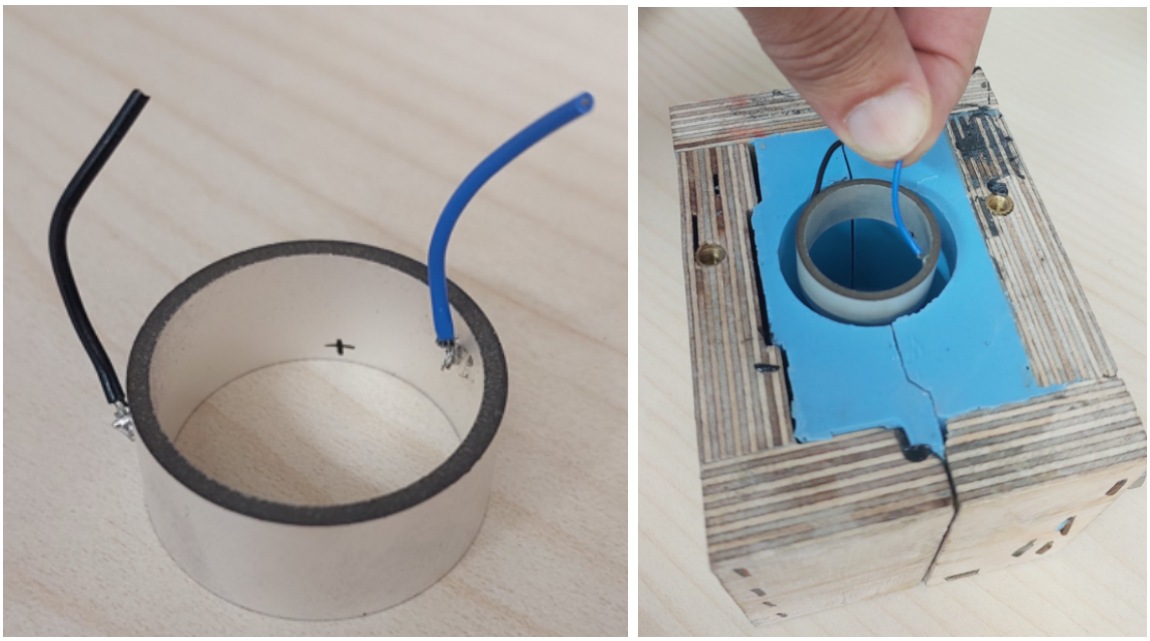

Fig. 9: Hydrophone production steps: preparing the piezoelectric element (left) and potting the hydrophone (right).

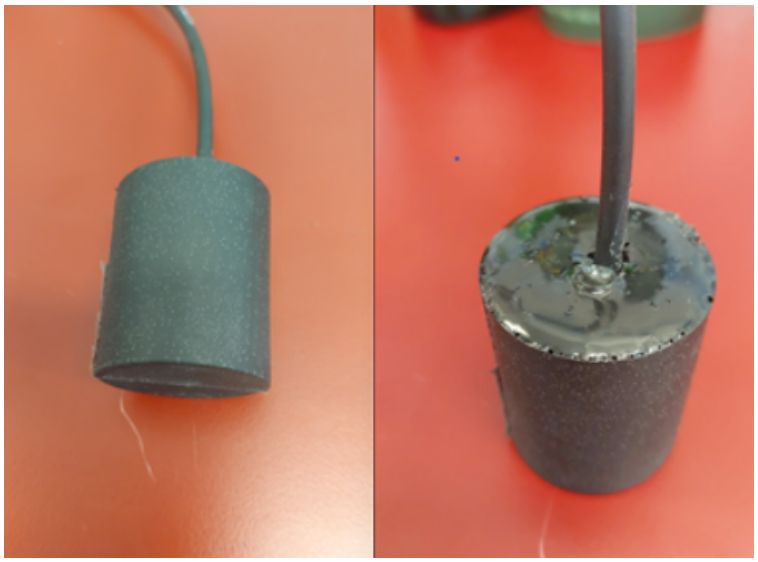

Fig. 10: Completed hydrophone for the SOUND floater.

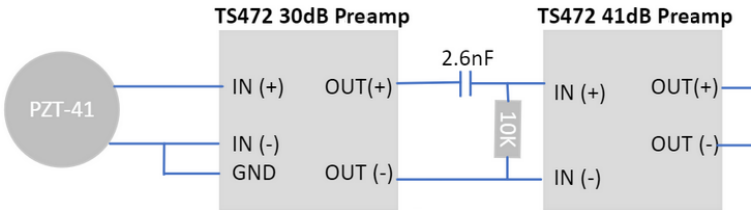


Fig. 11: Pre-amplifier connected to piezoelectric element.

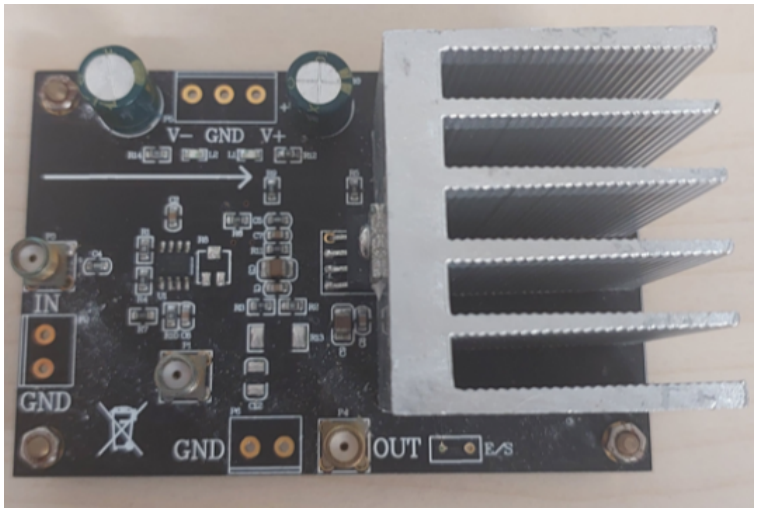


Fig. 12: SOUND floater acoustic subsystem amplifier.

*2) Amplifiers:*

The preamplifier consists of two TS472 boards, as shown in Fig. 11. It was designed for a low noise of $10nV/\sqrt{\text{Hz}}$ with an equivalent input noise at 1 kHz. It is a fully differential input/output circuit with a power consumption at 20 dB of 1.8 mA and a distortion of 0.1%. A high- pass filter at 5.9 KHz is integrated to avoid low-frequency noise and improve SNR.

The power amplifier used in the system is the OPA548 board shown in Fig. 12. The output impedance was adapted to the PZT41. The impedance matching circuit was calculated using the capacitance and resistance of the PZT41 at 30 KHz. The result is a 54 V peak-to-peak transmission when supplied with $\pm$28 VDC.

*3) Data Acquisition:*

The data acquisition (DAQ) component uses the OCTO sound card. This card comprises 6 input channels and 8 output channels, of which 4 inputs and 1 output are used. The channels can be sampled at up to 192 ksps at 24 bit. An isolated ADC and DAC help to reduce noise and

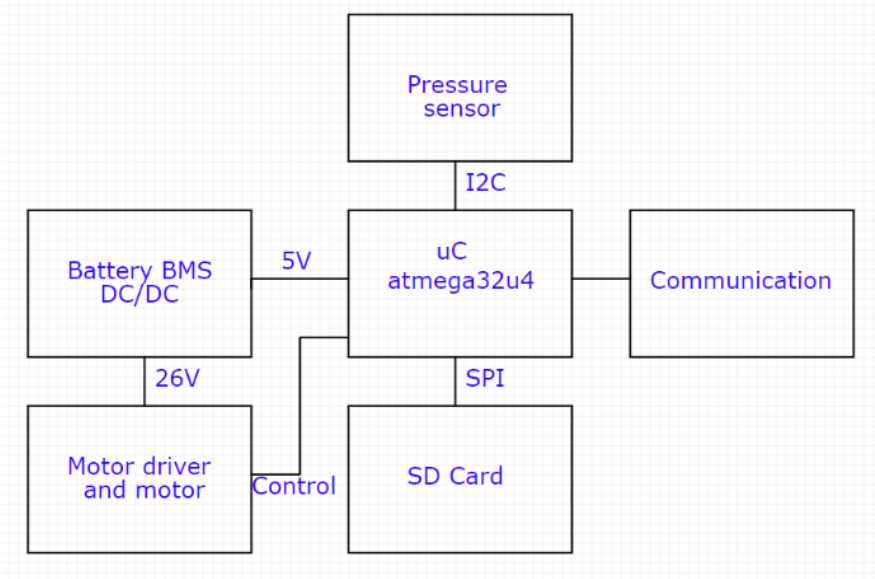


Fig. 13: Block diagram of the SOUND floater PCB internal communication protocols.

crosstalk. The sound card connects directly to the Raspberry Pi via a standard 40-pin header, with the GPIO lines broken out to control the preamp. The card has a full scale peak-to-peak output and input voltage of 4.8 V and 5.65 V, respectively, and a closed loop gain of -1.42 dB.

### *B. Depth control subsystem*

The block diagram of the PCB communication of the depth control subsystem is shown in Fig. 13. The PCB itself with all the main components highlighted is shown in Fig. 14. The main board contains an interface for an acoustic modem with receive/transmit capabilities for communication, a microSD card for data logging and a real-time clock (RTC) module. For depth control, the floater contains an MS5837-30BA pressure/temperature sensor with a resolution of 2 mm and an operating depth of up to 300 m. The TMC2208 stepper motor driver controls the 17HS19-1684S-PG5 stepper motor with high precision and ensures that the piston moves by 0.2 mm for each revolution of the motor.

The floater is operated with two battery packs. A battery management system (BMS) is responsible for balancing the cell load and managing the charging process. The cells used are Sony US18650VTC6 Li-ion battery cells. A single cell has 3000 mAh and a nominal voltage of 3.7 V. For the depth control board, the battery configuration is a single power supply consisting of $2 \times 7$ cells connected in series with a nominal voltage of 25.9 V and a capacity of 6000 mAh,

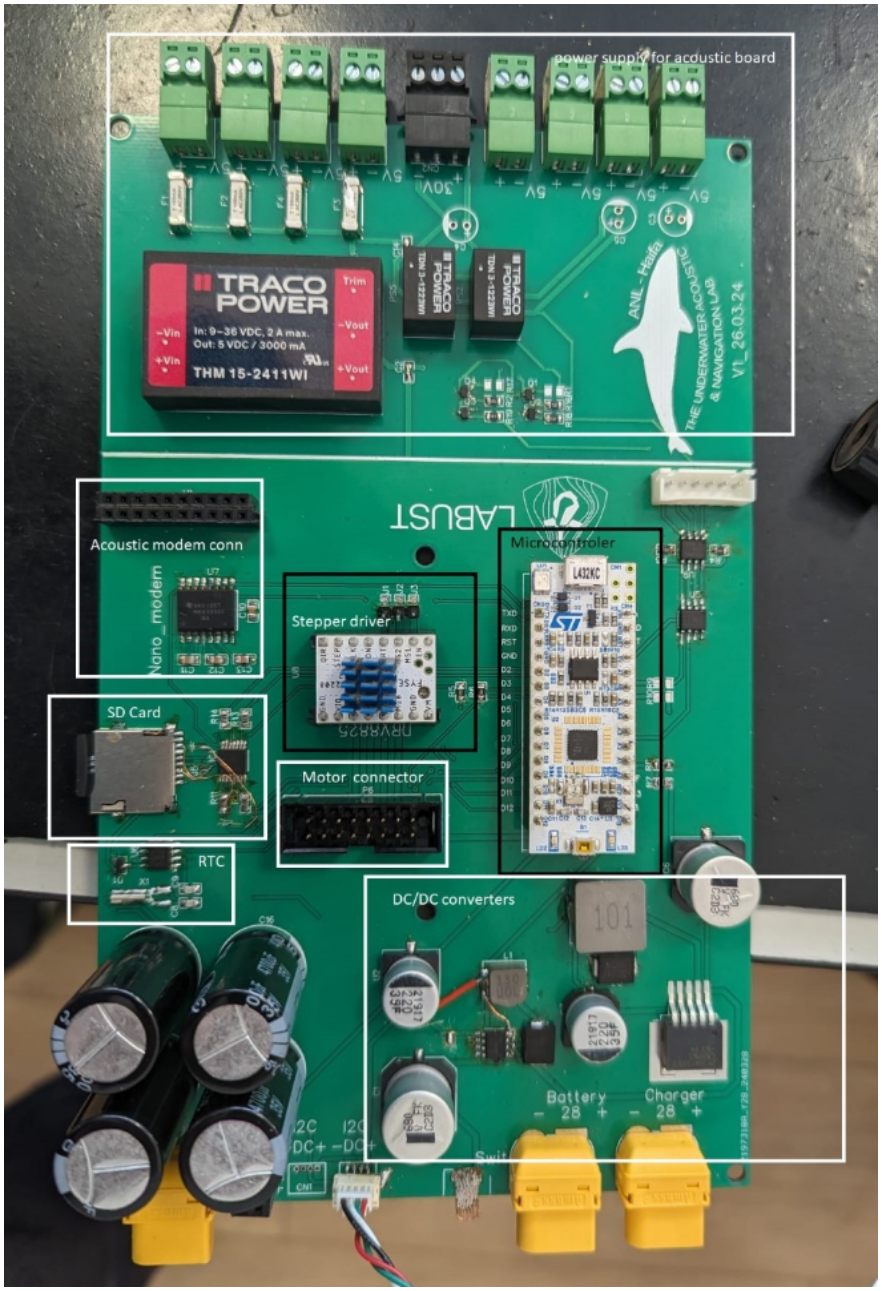


Fig. 14: SOUND floater main PCB.

giving 155 WH. For the acoustic subsystem, a dual power supply consisting of $1 \times 14$ cells connected in series for a nominal voltage of $\pm 25.9$ V and a capacity of 3000 mAh is provided, resulting in 155 WhH. Finally, two rotary switches are installed to switch the acoustic and control boards on and off independently.

# IV. Software and algorithmic design

The floater's main loop runs on the Arduino Micro, while the Raspberry Pi 4 goes through a sleep/wake cycle to conserve power and wakes up when its advanced processing capabilities are needed. The basic communication structure between the Raspberry Pi and the Arduino subsystems within a single floater, as well as the exchange of information between different floaters in the swarm, are illustrated in Fig. 15.

Controlled descent and ascent for vertical profiling is achieved by moving the piston from a neutrally buoyant position defined by an encoder offset. To reduce motor activity, we target the displacement of the piston to a minimum negative or minimum positive buoyancy, as the speed of movement is not a priority. During operation, the floater is initially trimmed so that the neutral buoyancy corresponds to a piston position where the piston bottom being flush with the lower edge of the floater hull.

## *A. Acoustic Detection*

The goal of the acoustic detection section of the SOUND floater is to detect multiple targets up to 500 m away, track their trajectory, estimate their biomass and determine their bearing. For this purpose, we have developed an active acoustic system with an omnidirectional projector and a planery array of 4 hydrophones. The projector emits a sequence of linear broadband chirp signals with a duration of 10 msc and a frequency band of 30 kHz-41 kHz. The chirp signals are sent at 0.7 sec intervals to allow reverberation up to 500 m away before the next transmission occurs. Each chirp signal is received synchronously by the 4 hydrophones and resampled after baseband conversion in the Rasberi Pi 4 unit. Detection is performed for a sliding window of 20 such chirp emissions.

The development of the acoustic detection system involves a novel detection algorithm that takes into account the temporal and spatial changes of the fish during detection. The algorithm creates a 3D matrix from temporal-spatial observations. The temporal domain is the reverberation received from the 20 emitted chirp signals. The spatial domain includes both distance and angle estimates. The former is obtained by a normalized matched filter (cf. [31]) and measuring the arrival time difference and multiplying it by the speed of sound speed, which is estimated from depth and temperature measurements on board the floater and a sound speed model. The latter is evaluated via beamforming performed for the 4 receiving channels. As the receiving array is planar, only the horizontal angle (heading) is estimated. The information from the gyrocompass

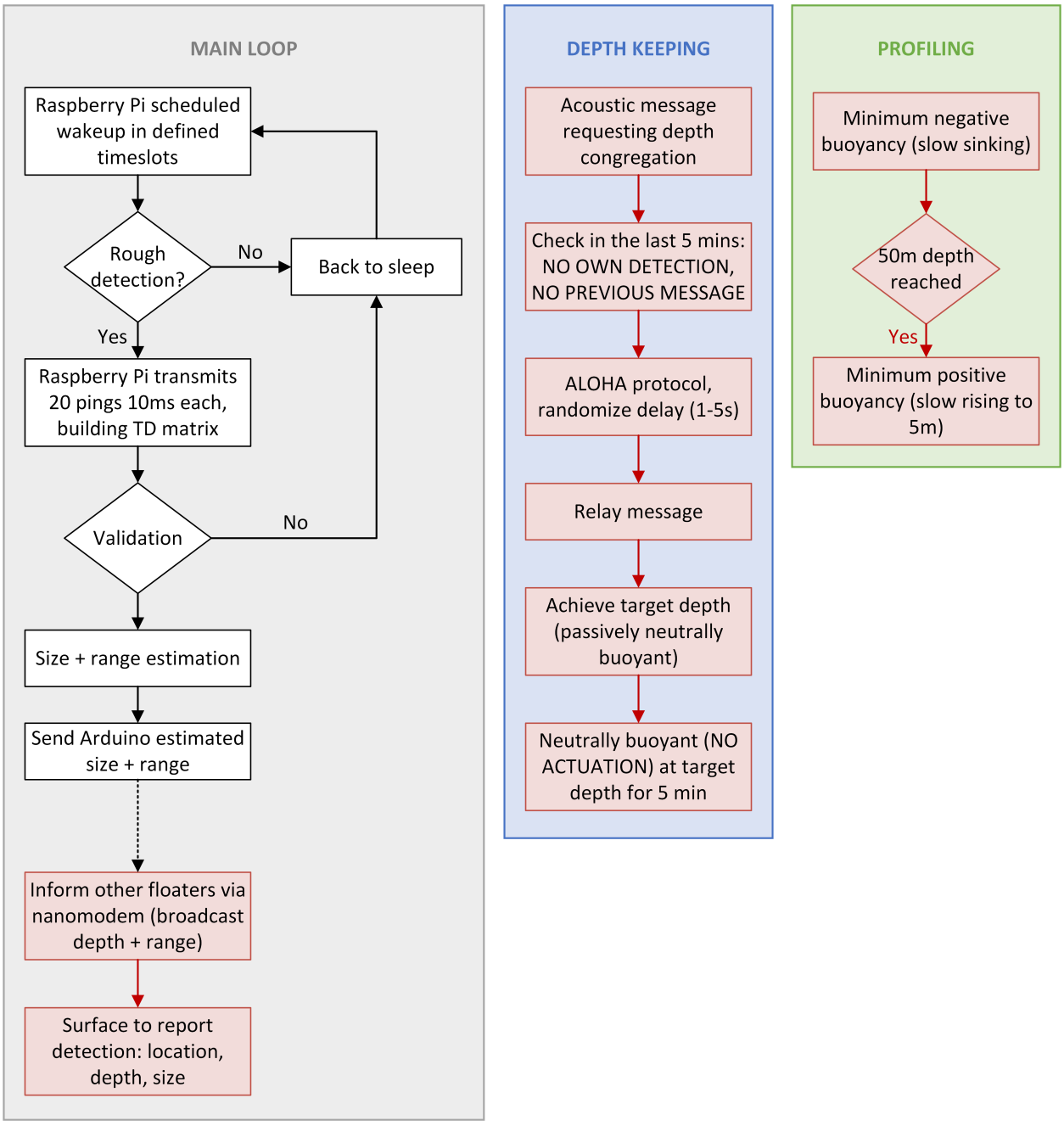


Fig. 15: Block diagram for the operation of the SOUND floater.

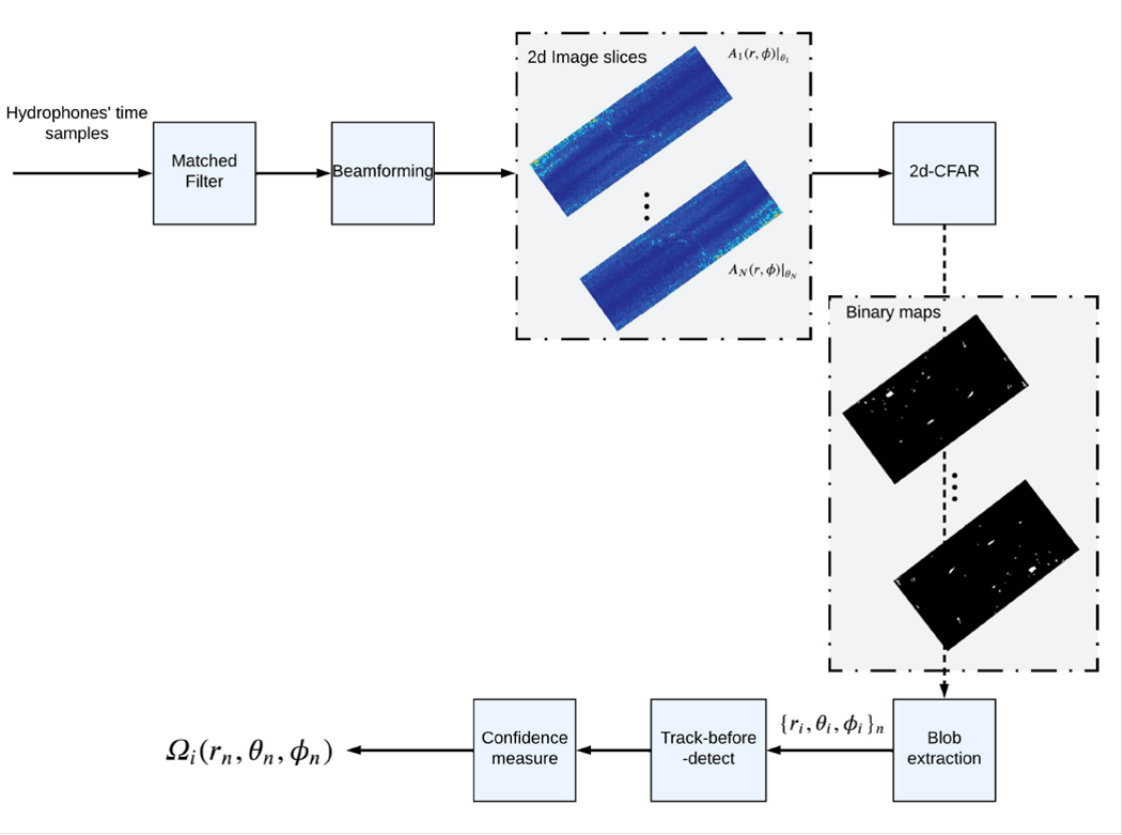


Fig. 16: Block diagram for the acoustic detection process.

is used here to align the measurements with true north and to compensate for any pitch or roll angles of the floater. Beamforming is performed after the matched-filter operation to compensate for the expected low clutter-to-noise ratio (CSR). The resulting 3D matrix is then clustered to find blobs of moving targets, which are the input for a Kalman-based multi-target tracker in the context of track-before-detect filtering. A confidence measure declares detection based on a stability test. The process is illustrated in Fig. 16, taken from [32], where more details about the acoustic detection part are available.

## V. Field experiments

### A. Laboratory conditions

The operation of the floater was validated in laboratory conditions in the LABUST laboratory pool in Zagreb, Croatia. The floater was trimmed to be approximately neutrally in the pool, tied to a rope and released. It was then acoustically instructed to sink, maintain depth and surface within the available depth of 3 m (Fig. 17).

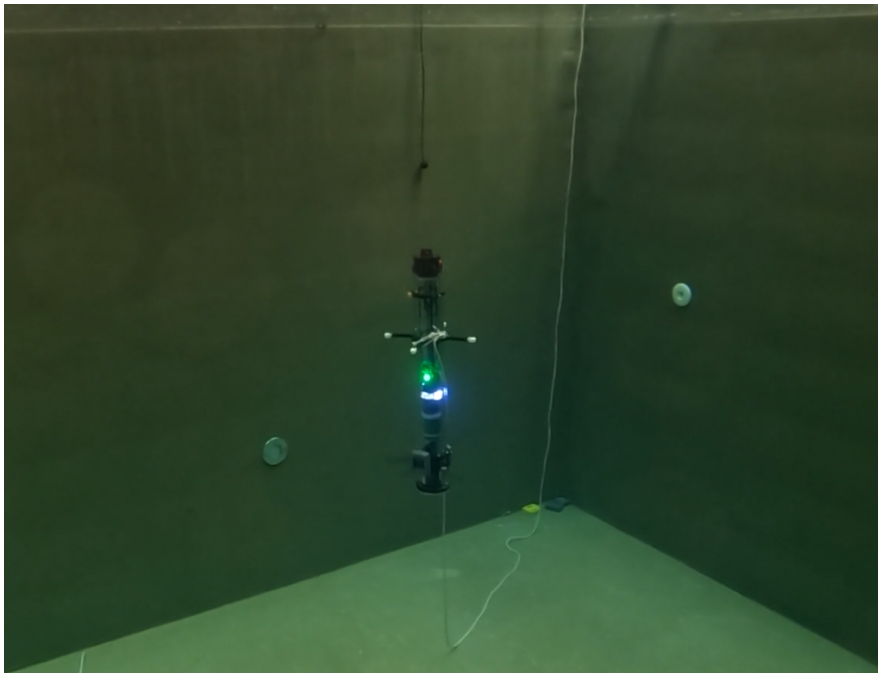

Fig. 17: SOUND floater performing depth-keeping in laboratory pool conditions.

Fig. 18: A photo of the SOUND floater prototype at 20m depth deployed in Eilat, Israel, July 2023. Picture taken by Mr. Liav Nagar.

### *B. Field Trials for Floater Design*

Two field trials were carried out to test the operation of the floater. To test the sensitivity to the marine environment, two marine environments were considered: the Red Sea and the Adriatic

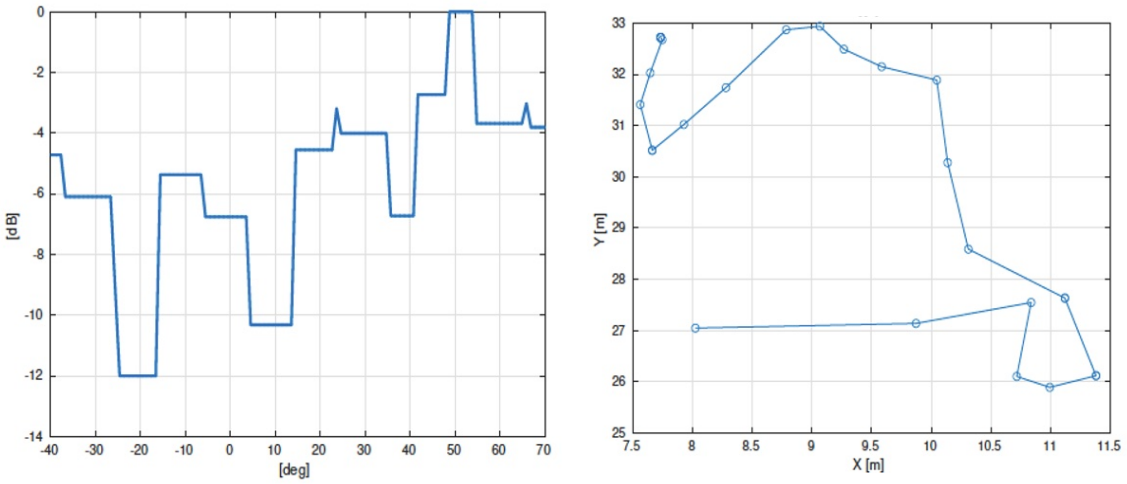


Fig. 19: Results of the acoustic detection tests in Eilat. Left panel: angle estimation. Right panel: location estimation. Track meets the location of the scuba diver with average error of roughly 5 m (against GPS).

Sea.

*1) Red Sea:* Sea trials were carried out in July 2023 to test floater operation under realistic conditions. After integration in laboratory facilities in Haifa, Israel, and a pressure chamber test for the required maximum depth of 50 m, field tests were conducted in Eilat, Israel, where the bathymetry is steep and allows easy access to a variety of depths (Fig. 18).

The field experiments included autonomous operation of a predefined mission. The floater was to maintain a specific depth for 30 minutes and then surface for recovery. Two divers followed the operation of the floater, and an operator on a pier remained in contact with the floater via acoustic communication. The deployment cycle (maintaining depth and then surfacing) was successfully completed. This mode of operation, including on-the-fly mission selection, will serve as the basis for the behavior of the SOUND floaters.

The experiment in the Red Sea for acoustic detection was conducted in 400 m water depth, an area with little fish population, to avoid unexpected targets. The floater was deployed to a depth of 12 m and kept at this depth. A pair of scuba divers served as targets. The position of the divers was monitored with a GPS logger attached to a small rubber buoy, which was attached to the divers with a fishing line. For safety reasons, the divers remained close to the vessel. The results of this operation are shown in Fig. 19 in terms of the angle estimate per chirp emission

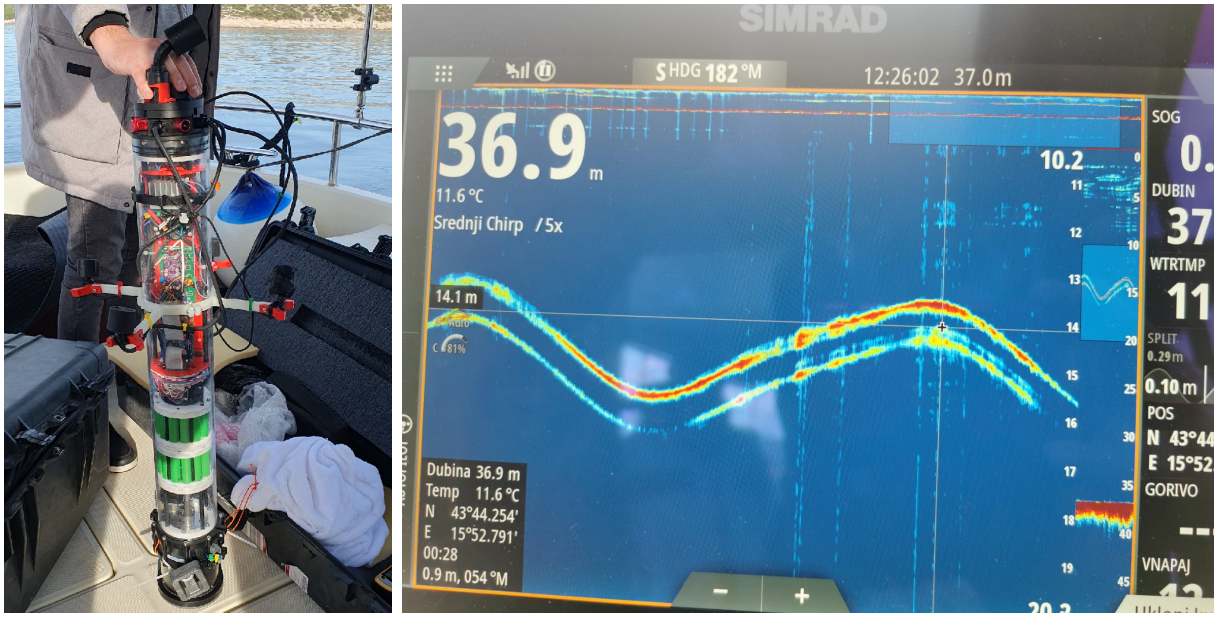


Fig. 20: SOUND floater prepared for deployment in Šibenik, Croatia, March 2024 (left). Floater oscillations around 15 m visible in the ship echosounder (right).

and the evaluated target trajectory (recall that our tracking is only performed on the horizontal plane). The track matched the diver's position with an average error of roughly 5 m.

*2) Adriatic Sea:* The acoustic detection in this sea experiment involved two target gilthead sea bream (*sparus aurata*) that were attached to buoys with a 20 m fishing line, similar to the pair of divers in the Red Sea experiment. A GPS logger was attached to each buoy to determine its position. Due to the length of the line to the fish, the GPS recording provided an accuracy of 20 m for the true location of the fish. The two fish were released close to the floater and then swam freely without directional restriction. The floater was set to maintain its position at a depth of 20 m. The procedure lasted 10 min, after which the fish were released. Ethical approval for this experiment was obtained from the Ruđer Bošković Institute, Croatia, and the experiments were conducted in accordance with EU ethical regulations. The methods used followed the ARRIVE guidelines (https://arriveguidelines.org). The results of this experiment are analyzed in [32] and presented in Fig. 21 for completeness. Errors within the GPS accuracy are observed.

## VI. Conclusions and Future Work

In this paper, we have presented the design details of a working, low-cost Lagrangian floater prototype intended for in situ monitoring of fish populations. The floater has active acoustic

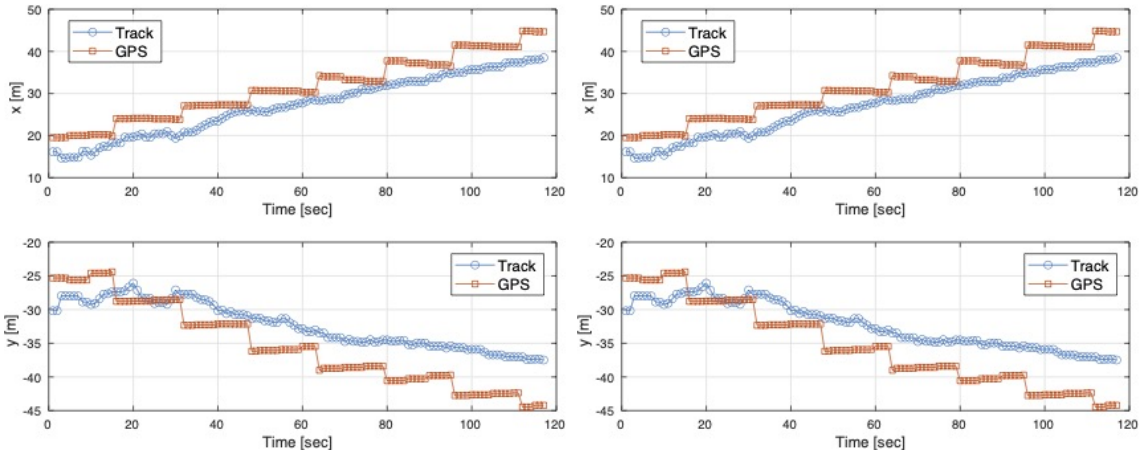


Fig. 21: Acoustic detection results from the experiment in the Adriatic Sea. Trajectory in the x-y plane estimated separately for two target fish swimming freely at the same time near the floater. Ground truth GPS-based location of the fish (20 m error) is marked in red.

detection capabilities and can profile the water column to a depth of 50 m or maintain depth while scanning its surroundings for schools of fish up to 500 m away. The prototype has been tested both in a laboratory pool and under field conditions. The buoyancy mechanism was redesigned with a focus on increasing robustness and replacing DC motors with stepper motors for more precise position control. Analysis of acoustic detection revealed several fish trajectories that were consistent enough to infer real targets. Finally, a long-term stress test of the floater will be conducted to ensure that it can meet the requirements for a 5-day operation.

## REFERENCES

[1] B. Worm, E. B. Barbier, N. Beaumont, J. E. Duffy, C. Folke, B. S. Halpern, J. B. Jackson, H. K. Lotze, F. Micheli, S. R. Palumbi, E. Sala, K. A. Selkoe, J. J. Stachowicz, and R. Watson, "Impacts of biodiversity loss on ocean ecosystem services," *Science*, vol. 314, no. 5800, pp. 787–790, Nov 2006.

[2] E. Josse and A. Bertrand, "In situ acoustic target strength measurements of tuna associated with a fish aggregating device," *ICES Journal of Marine Science*, vol. 57, no. 4, pp. 911–918, Aug 2000.

[3] E. K. Pikitch, C. Santora, E. A. Babcock, A. Bakun, R. Bonfil, D. O. Conover, P. Dayton, P. Doukakis, D. Fluharty, B. Heneman *et al.*, "Ecosystem-based fishery management," pp. 346–347, 2004.

[4] R. Curtin and R. Prellezo, "Understanding marine ecosystem based management: a literature review," *Marine policy*, vol. 34, no. 5, pp. 821–830, 2010.

[5] R. Diamant, "Concept of sound project," https://www.youtube.com/watch?v=lcO53wWfBmQ&embeds$_$referring$_$euri=https%3A%2F%2Fsites.google.com%2F&feature=emb_imp$_$woyt, April 2024.

[6] A. Bertrand and E. Josse, "Acoustic estimation of longline tuna abundance," *ICES Journal of Marine Science*, vol. 57, no. 4, pp. 919–926, 2000.

[7] T. B. Letessier, P. J. Bouchet, and J. J. Meeuwig, "Sampling mobile oceanic fishes and sharks: implications for fisheries and conservation planning," *Biological Reviews*, vol. 92, no. 2, pp. 627–646, 2017.

[8] J. Aguzzi, N. Iveša, M. Gelli, C. Costa, A. Gavrilovic, N. Cukrov, M. Cukrov, N. Cukrov, D. Omanovic, M. Štifanić *et al.*, "Ecological video monitoring of marine protected areas by underwater cabled surveillance cameras," *Marine policy*, vol. 119, p. 104052, 2020.

[9] M. J. Parsons, I. M. Parnum, K. Allen, R. D. McCauley, and C. Erbe, "Detection of sharks with the gemini imaging sonar," *Acoust. Aust*, vol. 42, no. 3, pp. 185–190, 2014.

[10] N. Kapetanović, A. Vasilijević, Đ. Nađ, K. Zubčić, and N. Mišković, "Marine robots mapping the present and the past: Unraveling the secrets of the deep," *Remote sensing*, vol. 12, no. 23, p. 3902, 2020.

[11] S. Gonzalez, A. Gonzalez-Briones, A. Gola, G. Katranas, M. Ricca, R. Loukanova, J. Prieto *et al.*, "Preface-advances in intelligent systems and computing," *ADVANCES IN INTELLIGENT SYSTEMS AND COMPUTING*, vol. 1242, pp. v–vi, 2021.

[12] N. Kapetanović, B. Kordić, A. Vasilijević, Đ. Nađ, and N. Mišković, "Autonomous vehicles mapping plitvice lakes national park, croatia," *Remote sensing*, vol. 12, no. 22, p. 3683, 2020.

[13] C. Jiang, J. Li, and W. Xu, "The use of underwater gliders as acoustic sensing platforms," *Applied Sciences*, vol. 9, no. 22, p. 4839, 2019.

[14] D. Guihen, "High-resolution acoustic surveys with diving gliders come at a cost of aliasing moving targets," *Plos one*, vol. 13, no. 8, p. e0201816, 2018.

[15] M. Wei, B. Shi, C. Hao, and S. Yan, "A novel weak target detection strategy for moving active sonar," in *2018 OCEANS-MTS/IEEE Kobe Techno-Oceans (OTO)*. IEEE, 2018, pp. 1–6.

[16] J. R. Bates, D. Grimmett, G. Canepa, and A. Tesei, "Towards doppler estimation and false alarm rejection for continuous active sonar," *The Journal of the Acoustical Society of America*, vol. 143, no. 3_Supplement, pp. 1972–1972, 2018.

[17] R. Baran, T. Juza, M. Tuser, H. Balk, P. Blabolil, M. Cech, V. Drastik, J. Frouzova, A. D. Jayasinghe, I. Koliada *et al.*, "A novel upward-looking hydroacoustic method for improving pelagic fish surveys," *Scientific reports*, vol. 7, no. 1, p. 4823, 2017.

[18] M. Barra, A. Bonanno, T. Hattab, C. Saraux, M. Iglesias, I. Leonori, V. Ticina, G. Basilone, A. De Felice, R. Ferreri *et al.*, "Effects of sampling intensity and biomass levels on the precision of acoustic surveys in the mediterranean sea," *Mediterranean Marine Science*, vol. 22, no. 4, pp. 769–783, 2021.

[19] J. Wanzenböck, J. Kubecka, Z. Sajdlova, and J. Frouzova, "Hydroacoustic target strength vs. fish length revisited: Data of caged, free-swimming european whitefish (coregonus lavaretus l.) suggest a bi-phasic linear relationship under a limited range of tilt angles," *Fisheries research*, vol. 229, p. 105620, 2020.

[20] C. de MOUSTIER, "State of the art in swath bathymetry survey systems," 1988.

[21] S. R. Jayne, D. Roemmich, N. Zilberman, S. C. Riser, K. S. Johnson, G. C. Johnson, and S. R. Piotrowicz, "The Argo program: Present and future," *Oceanography*, vol. 30, no. 2, pp. 18–28, Jun 2017.

[22] T. B. Sanford, J. H. Dunlap, J. A. Carlson, D. C. Webb, and J. B. Girton', "Autonomous velocity and density profiler: EM-APEX," in *Proceedings of the IEEE Working Conference on Current Measurement Technology*. IEEE, 2005, pp. 152–156.

[23] L. K. Shay, J. K. Brewster, B. Jaimes, C. Gordon, K. Fennel, P. Furze, H. Fargher, and R. He, "Physical and Biochemical Structure Measured by APEX-EM Floats," in *2019 IEEE/OES 12th Current, Waves and Turbulence Measurement, CWTM 2019*. IEEE, Mar 2019, pp. 1–6.

[24] M. F. de Jong, H. Søiland, A. S. Bower, and H. H. Furey, "The subsurface circulation of the Iceland Sea observed with RAFOS floats," *Deep-Sea Research Part I: Oceanographic Research Papers*, vol. 141, pp. 1–10, Nov 2018.

391 [25] J. S. Jaffe, P. J. Franks, P. L. Roberts, D. Mirza, C. Schurgers, R. Kastner, and A. Boch, "A swarm of autonomous miniature
392 underwater robot drifters for exploring submesoscale ocean dynamics," *Nature Communications*, vol. 8, no. 1, p. 14189,
393 Jan 2017.
394 [26] Y. Katz and M. Groper, "On the Development of a Mid-Depth Lagrangian Float for Littoral Deployment," *Journal of*
395 *Marine Science and Engineering*, vol. 10, no. 12, p. 2030, Dec 2022.
396 [27] I. Klein and R. Diamant, "Dead reckoning for trajectory estimation of underwater drifters under water currents," *Journal*
397 *of Marine Science and Engineering*, vol. 8, no. 3, p. 205, Mar 2020.
398 [28] Y. Hoffman, L. Nagar, I. Shachar, and R. Diamant, "A Simple Approach to Estimate the Drag Coefficients of a Submerged
399 Floater," *Sensors*, vol. 23, no. 3, p. 1394, Jan 2023.
400 [29] A. Babić, I. Lončar, B. Arbanas, G. Vasiljević, T. Petrović, S. Bogdan, and N. Mišković, "A Novel Paradigm for Underwater
401 Monitoring Using Mobile Sensor Networks," *Sensors*, vol. 20, no. 16, p. 4615, Aug 2020.
402 [30] D. Fenucci, J. Sitbon, J. Neasham, A. Phillips, and A. Munafò, "Ad hoc acoustic network aided localization for micro-
403 AUVs," *Field Robotics*, vol. 2, no. 1, pp. 1888–1919, 2022.
404 [31] R. Diamant, "Closed form analysis of the normalized matched filter with a test case for detection of underwater acoustic
405 signals," *IEEE Access*, vol. 4, pp. 8225–8235, 2016.
406 [32] A. Abu, N. Miskovic, O. Chebotar, N. Cukrov, and R. Diamant, "Multiple mobile target detection and tracking in active
407 sonar array using a track-before-detect approach," arXiv:2404.10316, April 2024.